Available online at www.sciencedirect.com
SCIENCE DIRECT
Solid State Communications 138 (2006) 534–537
solid state communications
www.elsevier.com/locate/ssc

# High-pressure formation of $Mg_xZn_{1-x}O$ solid solutions with rock salt structure

Vladimir L. Solozhenko [a,*], Andrey N. Baranov [b], Vladimir Z. Turkevich [c]

[a] LPMTM-CNRS, Institut Galilée, Université Paris Nord, 99, av. J.B. Clément, 93430 Villetaneuse, France
[b] Chemistry Department, Moscow State University, 119992 Moscow, Russian Federation
[c] Institute for Superhard Materials of the National Academy of Sciences of Ukraine, 04074 Kiev, Ukraine

Received 28 November 2005; received in revised form 10 April 2006; accepted 12 April 2006 by R. Phillips
Available online 4 May 2006

**Abstract**

X-ray diffraction with synchrotron radiation has been used for the first time to study the formation of $Mg_xZn_{1-x}O$ (MZO) ($0.33 \le x \le 0.83$) solid solutions with rock salt structure at pressures up to 4.4 GPa and temperatures up to 1500 K. The chemical reaction between MgO and ZnO and a subsequent phase transformation of wurtzite solid solution (w-MZO) into rock salt one (rs-MZO) was observed at a stepwise heating at various pressures. The lattice parameters of rs-MZO solid solutions of different stoichiometries have been in situ measured at high pressures and temperatures. Unlike pure ZnO, the quenching of the reaction mixtures resulted in the formation of stabile MZO solid solutions with the rock salt structure. The phase diagram of the MgO–ZnO system at 4.4 GPa has been proposed based on the experimental data.


*PACS:* 61.10.Eq; 64.70.Kb

*Keywords:* A. Semiconductors; D. Phase transition; D. High pressure; E. Synchrotron radiation

## 1. Introduction

The zinc oxide is a semiconductor with wide band gap ($E_g = 3.37$ eV) and large exciton binding energy. ZnO heterostructures with MgO ($E_g \sim 7.5$ eV) have drawn world-wide attention due to the possible applications in electronics, e.g. short-wavelength display diodes and room-temperature UV lasers [1]. The MgO–ZnO solid solutions (MZO) allow tailoring of the direct bandgap materials into extremely short wavelength regions. A large number of attempts aimed at extending the bandgap of ZnO by alloying with MgO have been reported [2–10].

At ambient conditions, the MgO–ZnO system is of eutectic type and is characterized by an extensive solubility of ZnO in MgO and a restricted solubility of MgO in ZnO, though the solubility is temperature dependent. The two-phase region in the MgO–ZnO system extends from 3.5 to 70.5 mol% ZnO at 1000 °C and becomes narrower at higher temperatures [11].

In situ synchrotron radiation studies have shown that at room temperature the reversible transformation from wurtzite to rock salt phase in ZnO occurs at about 9 GPa [12–17]. Upon decompression down to 2 GPa, the rock salt phase reverts to the wurtzite one. Large pressure hysteresis results from the kinetic limitations at room temperature. Phase boundary between the wurtzite and rock salt phases has been defined as the $P$ (GPa) $= 6.1 - 0.0012 \times T$ (°C) straight line [17].

Previously, we have studied the MgO–ZnO system at high pressures and temperatures by quenching and found that the rock salt MZO phase can be stabilized over the wide concentration range [10]. The use of X-ray diffraction with synchrotron radiation allows in situ observation of chemical reactions and phase transitions at high pressures and temperatures [18–20]. Here, we report the first synchrotron radiation study of the formation of rock salt $Mg_xZn_{1-x}O$ ($0.33 \le x \le 0.83$) solid solutions at high pressures and temperatures.

## 2. Experimental

Reaction mixtures of ZnO and MgO have been prepared from hydroxide carbonates as described previously [10]. As-prepared mixtures were uniaxially compressed into

* Corresponding author. Tel.: +33 1 49 40 34 89; fax: +33 1 49 40 3938.
*E-mail address:* vls@lpmtm.univ-paris13.fr (V.L. Solozhenko).

0038-1098/$ - see front matter © 2006 Elsevier Ltd. All rights reserved.
doi:10.1016/j.ssc.2006.04.005

Table 1
Compositions of reaction mixtures

| | $x$ | Composition |
|---|---|---|
| MZO1 | 0.32 | $Mg_{0.32}Zn_{0.68}O$ |
| MZO2 | 0.68 | $Mg_{0.68}Zn_{0.32}O$ |
| MZO3 | 0.83 | $Mg_{0.83}Zn_{0.17}O$ |

cylindrical disks and placed into capsules of high-purity hexagonal graphite-like boron nitride. The high-pressure experiments were carried out using the multianvil X-ray system MAX80. The diffraction measurements were performed in an energy-dispersive mode at the beamline F2.1, HASYLAB-DESY. X-ray patterns were collected on a Canberra solid state Ge-detector with fixed Bragg angle $2\theta = 9.260(3)°$. The temperature of the high-pressure cell was controlled by a Eurotherm PID regulator within 2 K. Pressures at different temperatures were calculated from lattice parameters of hBN using its thermoelastic equation of state [18]. The details of experiments and high-pressure setup have been described earlier [18–20]. At first, the samples were compressed to a given pressure at ambient temperature, and then the energy-dispersive diffraction patterns were in situ collected at stepwise (at a step of 25–50 K) heating at fixed pressure. The time of data collection for each pattern was about 5 min. The compositions of reaction mixtures are shown in Table 1.

## 3. Results and discussion

Synchrotron radiation patterns of the initial reaction mixtures exhibit only lines of ZnO (S.G. $P6_3/mc$ (186); ICDD PDF2 card 36-1451) and MgO (S.G. $Fm3m$ (225); ICDD PDF2 card 45-0946), no other lines have been detected. This fact indicates that no MZO solid solutions have formed during the preparation of the reaction mixtures.

Characteristic diffraction patterns taken from the MZO2 sample at 4.4 GPa and different temperatures are shown in Fig. 1. It should be noted that unusual line intensity ratio observed experimentally is due to the special features of the used energy-dispersive technique, i.e. high-pressure cell absorption, spectral distribution of brilliance of the synchrotron radiation source, limited reciprocal space covered by the zero-dimensional Ge-detector and energy dependence of its quantum efficiency. Diffraction lines of rs-MZO are indexed by underlined numerals while indexes for wurtzite ZnO are not underlined. Some of the lines (e.g. 101 and 111) are overlapped and not resolved.

At 4.4 GPa, heating of the ZnO–MgO mixtures brings about the formation of two MZO solid solutions with the rock salt and wurtzite structures. The processes occurring with increasing temperature (in particular, the disappearance of 102 line of wurtzite ZnO and shift of 200 line of rs-MZO to higher $d$-spacings) are illustrated in more detail in Fig. 2. All these features are observed for all samples irrespective of the stoichiometry, though for reaction mixtures of lower MgO content they are shifted to higher temperatures (at given

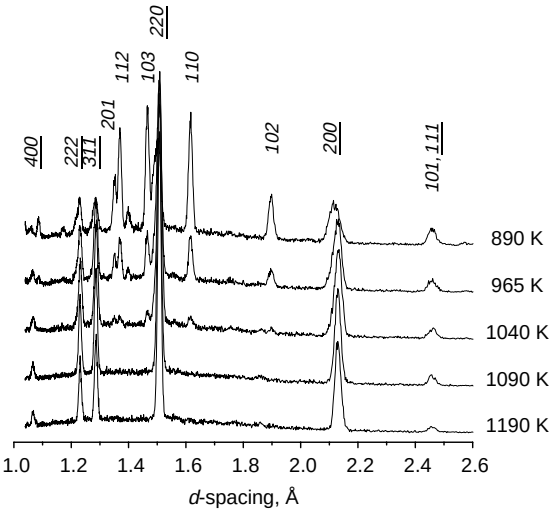


Fig. 1. Diffraction patterns of the MZO2 sample taken at 4.4 GPa in the course of stepwise heating.

pressure). Thus, for the MZO1, MZO2 and MZO3 samples, the complete disappearance of the w-ZnO lines is observed at 975, 1090 and 1350 K, respectively, and the diffraction patterns exhibit only lines of rs-MZO.

The temperature dependencies of the lattice parameters for all samples at 4.4 GPa are shown in Fig. 3. As it seen from the figure, all the curves consist of two parts: exponential and linear. Exponential growth of the lattice parameters at low temperatures corresponds to the dissolution of ZnO in the MgO lattice and the fast formation of the rs-MZO solid solutions. The end point of the exponential part corresponds the ultimate solubility of ZnO in MgO at given pressure and temperature and may be defined as a temperature of the w-MZO-to-rs-MZO phase transition ($T_{tr}$). The linear part of the curve is due to the thermal expansion of the as-formed rs-MZO solid solution, and its slope gives the value of the linear thermal expansion coefficient at a given pressure. The thermal expansion

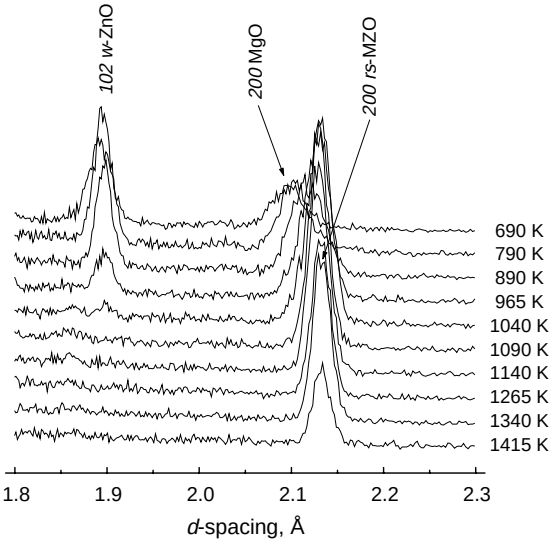


Fig. 2. Evolution of 102 line of wurtzite ZnO and 200 line of rs-MZO at 4.4 GPa upon stepwise heating up to 1415 K.

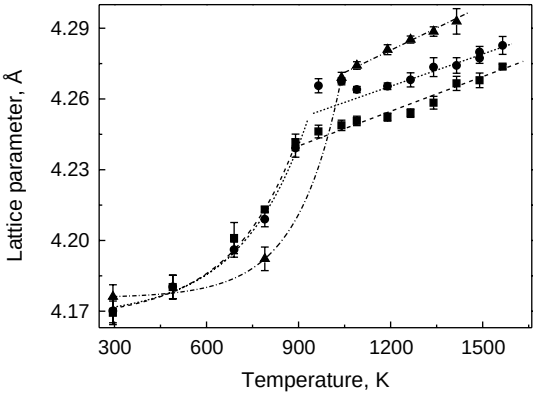


Fig. 3. Lattice parameters of rock salt MZO solid solutions vs. temperature at 4.4 GPa (triangles—MZO1, circles—MZO2, squares—MZO3).

coefficients for all the rock salt MZO solid solutions being studied are of the same order of magnitude as for pure MgO [21] (Table 2).

The temperature of the complete disappearance of the w-MZO phase ($T_{\text{w-MZO}}$) is higher than the onset temperature of the formation of the rs-MZO phase ($T_{\text{rs-MZO}}$). This difference is near the same for all reaction mixtures regardless of the stoichiometry as shown in Fig. 4. The extrapolation of the concentration dependence of $T_{\text{rs-MZO}}$ to $x=0$ gives the value close to the transition temperature calculated for pure ZnO at 4.4 GPa from the data reported in [17]. Thus, we can consider the dashed line in Fig.4 as a phase boundary between w-MZO and rs-MZO.

All the results obtained in our experiments have been used as the basis for the construction of the phase diagram of the MgO–ZnO system at 4.4 GPa presented in Fig. 5. The MgO stability region expands with pressure since the rock salt phase has the lowest molar volume in the system. At the same time, rock salt ZnO is stabilized at high pressures. As a result, at 4.4 GPa the diagram of the MgO–ZnO system is characterized by the region of rs-MZO unlimited solid solutions with rock salt ZnO. The w-MZO stability region is in low-temperature part of the diagram for ZnO-rich compositions. The rock salt and wurtzite phase regions are separated by the rs-MZO + w-MZO two-phase region, which corresponds to the experimentally observed w-MZO-to-rs-MZO phase transition. Since temperature of the w-MZO-to-rs-MZO transition is a linear function of composition, the solutions of the ZnO–MgO system are near-ideal. We suggest that after the evolution from the eutectic-type diagram at ambient pressure, the melting diagram of the MgO–ZnO system at 4.4 GPa has the shape and position presented in Fig. 5.

Table 2
Linear thermal expansion coefficients ($\alpha$) of rock salt MZO solid solutions at 4.4 GPa

| | $\alpha\times10^5$ ($K^{-1}$) |
|---|---|
| $Mg_{0.32}Zn_{0.68}O$ | $6.3\pm0.8$ |
| $Mg_{0.68}Zn_{0.32}O$ | $4.6\pm1.3$ |
| $Mg_{0.83}Zn_{0.17}O$ | $4.9\pm0.3$ |
| MgO | 4.07 [21] |

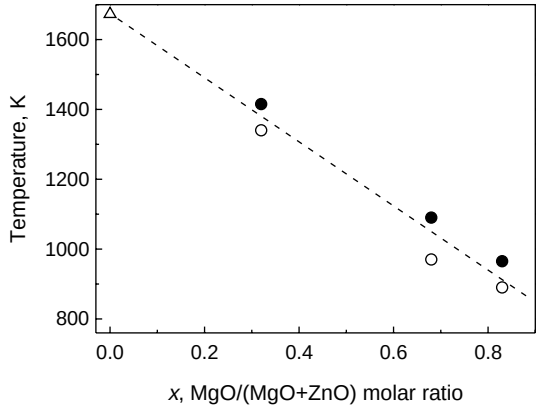


Fig. 4. Temperature of the rs-MZO phase formation vs. MgO/(MgO + ZnO) molar ratio $x$. Triangle—transition temperature calculated for pure ZnO at 4.4 GPa, open circles—temperature of rock salt MZO appearance, solid circles—temperature of the complete disappearance of 101 line of wurtzite MZO.

Thus, our findings have shown that under high pressures and temperatures MgO–ZnO mixtures undergo the chemical reaction and a subsequent phase transformation of the as-formed wurtzite MZO solid solution into the rock salt MZO solid solution by the following scheme

$$\text{MgO} + \text{ZnO} \rightarrow (\text{w-MZO} + \text{rs-MZO}) \rightarrow \text{rs-MZO}$$

The final product remains stable after quenching down to ambient conditions. The temperature of the w-MZO-to-rs-MZO phase transition depends on the MgO concentration $x$ and decreases linearly with increasing $x$. This transition occurs in the temperature range that corresponds to the w-MZO + rs-MZO two-phase region in the proposed phase diagram of the MgO–ZnO system at 4.4 GPa.

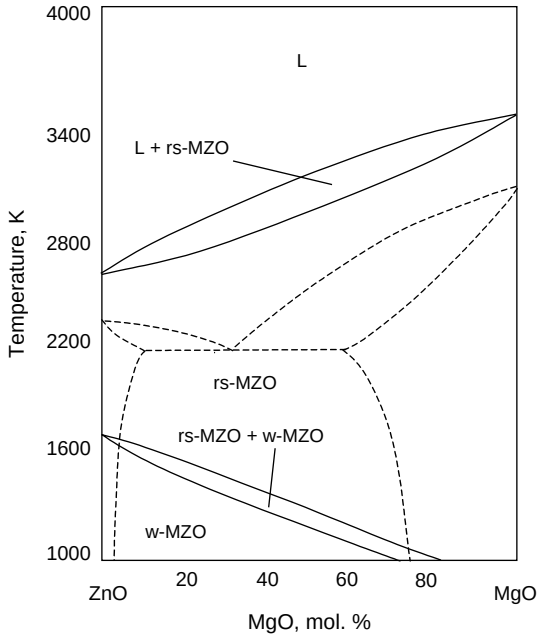


Fig. 5. Phase diagram of the MgO–ZnO system at 4.4 GPa (solid line) and at ambient pressure [11] (dashed line).

## Acknowledgements

This work was supported by the GFZ-Potsdam under the MAX80 program. The authors thank Dr Ch. Lathe for assistance in high-pressures experiments and O.O. Kurakevich for discussion. A.N.B. has been receiving support from the Université Paris Nord and from the 'Rosnauka' under the project IN-12.5/002 (N02.434.11.2017) that are acknowledged with gratitude.

## References

[1] A. Ohtomo, M. Kawasaki, T. Koida, K. Masubuchi, H. Koinuma, Y. Sakurai, Y. Yoshida, T. Yasuda, Y. Segawa, Appl. Phys. Lett. 72 (1998) 2466.
[2] J. Chen, W.Z. Shen, N.B. Chen, D.J. Qiu, H.Z. Wu, J. Phys.: Condens. Matter 15 (2003) L475.
[3] W.I. Park, G.C. Yi, H.M. Jang, Appl. Phys. Lett. 79 (2001) 2022.
[4] J. Naryana, A.K. Sharma, A. Kvit, C. Jin, J.F. Muth, O.W. Holland, Solid State Commun. 121 (2002) 9.
[5] S. Choopun, R.D. Vispute, W. Yang, R.P. Sharma, T. Venkatesan, H. Shen, Appl. Phys. Lett. 80 (2002) 1529.
[6] I. Takeuchi, W. Yang, K.S. Chang, M.A. Aronova, T. Venkatesan, R.D. Vispute, L.A. Bendersky, J. Appl. Phys. 94 (2003) 7336.
[7] N.B. Chen, H.Z. Wu, D.J. Qiu, T.N. Xu, J. Chen, W.Z. Shen, J. Phys.: Condens. Matter 16 (2004) 2973.
[8] T. Gruber, C. Kirchner, R. Kling, F. Reuss, A. Waag, Appl. Phys. Lett. 84 (2004) 5359.
[9] M. Kunisu, I. Tanaka, T. Yamamoto, T. Suga, T. Mizoguchi, J. Phys.: Condens. Matter 16 (2004) 3801.
[10] A.N. Baranov, V.L. Solozhenko, C. Chateau, G. Bocquillon, J.P. Petitet, G.N. Panin, T.W. Kang, R.V. Shpanchenko, E.V. Antipov, Y.J. Oh, J. Phys.: Condens. Matter 17 (2005) 3377.
[11] S. Raghavan, J.P. Hajra, G.N.K. Iyengar, K.P. Abraham, Thermochim. Acta 189 (1991) 151.
[12] L. Gerward, J.S. Olsen, J. Synchrotron Rad. 2 (1995) 233.
[13] J.M. Recio, M.A. Blanco, V.L.R. Pandey, L. Gerward, J.S. Olsen, Phys. Rev. B 58 (1998) 8949.
[14] S. Desgreniers, Phys. Rev. B 58 (1998) 14102.
[15] J.Z. Jiang, J.S. Olsen, L. Gerward, D. Frost, D. Rubie, J. Peyronneau, Europhys. Lett. 50 (2000) 48.
[16] F. Decremps, J. Zhang, R.C. Liebermann, Europhys. Lett. 51 (2000) 268.
[17] K. Kusaba, Y. Syono, T. Kikegawa, Proc. Jpn. Acad., Ser. B 75B (1) (1999) 1.
[18] V.L. Solozhenko, T. Peun, J. Phys. Chem. Solids 58 (1997) 1321.
[19] A.N. Baranov, V.L. Solozhenko, C. Lathe, V.Z. Turkevich, Y.W. Park, Supercond. Sci. Technol. 16 (2003) 1147.
[20] V.L. Solozhenko, Y.L. Godec, S. Klotz, M. Mezouar, V.Z. Turkevich, J.M. Besson, Phys. Chem. Chem. Phys. 4 (2002) 5386.
[21] S. Gaurava, B.S. Sharmaa, S.B. Sharmab, S.C. Upadhyaya, J. Phys. Chem. Solids 65 (2004) 1635.